

Mean Free Path of Neutral Penetrating Shower-Producing Radiation*

H. W. BOEHMER†

Department of Physics, University of Colorado, Boulder, Colorado

AND

H. S. BRIDGE

Department of Physics and Laboratory for Nuclear Science and Engineering, Massachusetts Institute of Technology, Cambridge, Massachusetts

(Received November 2, 1951)

The collision mean free path has been measured in carbon and in lead for neutral particles capable of producing penetrating showers.

Several types of events are selected with different multiplicities of particles in the penetrating shower. For the events with highest multiplicity the mean free path is $85 \pm 12 \text{ g cm}^{-2}$ in carbon, and $143 \pm 30 \text{ g cm}^{-2}$ in lead.

INTRODUCTION

THE measurements reported here are a continuation of experiments on the production of charged secondaries by neutral particles in the cosmic radiation. This work was initiated by Rossi and Regener¹ and extended by Janosy and Rochester.² In principle, the method allows a determination of the collision mean free path for penetrating shower production by the neutral radiation. The present experiment was undertaken to improve the statistical accuracy of the previous results and to remove some of the uncertainties resulting from various sources of background. An experiment similar to this has been performed recently by Walker, Walker, and Greisen.³ Our results agree closely with theirs, but since the experimental conditions and methods of analysis are rather different, it seems

worthwhile to describe the present experiment in some detail.

EXPERIMENTAL METHOD

A schematic diagram of the apparatus is given in Fig. 1. The Geiger-Müller counters were of the metal type filled with an alcohol-argon self-quenching mixture. The effective area of each of the *A* tray counters was $1 \text{ in.} \times 20 \text{ in.}$ while that of the counters in the *B*, *C*, *D*, *E*, and *F* trays was $1 \text{ in.} \times 10 \text{ in.}$ Trays *B*, *C*, *D*, and *E* make up the penetrating shower detector. The counters in trays *B* and *E* were connected to addition circuits that made it possible to record coincidences of the type $B_m C D E_n$, wherein *m* or more counters were discharged in the *B* tray, one or more counters in the *C* and *D* trays, and *n* or more counters in the *D* tray. Normally the penetrating charged particles were required to

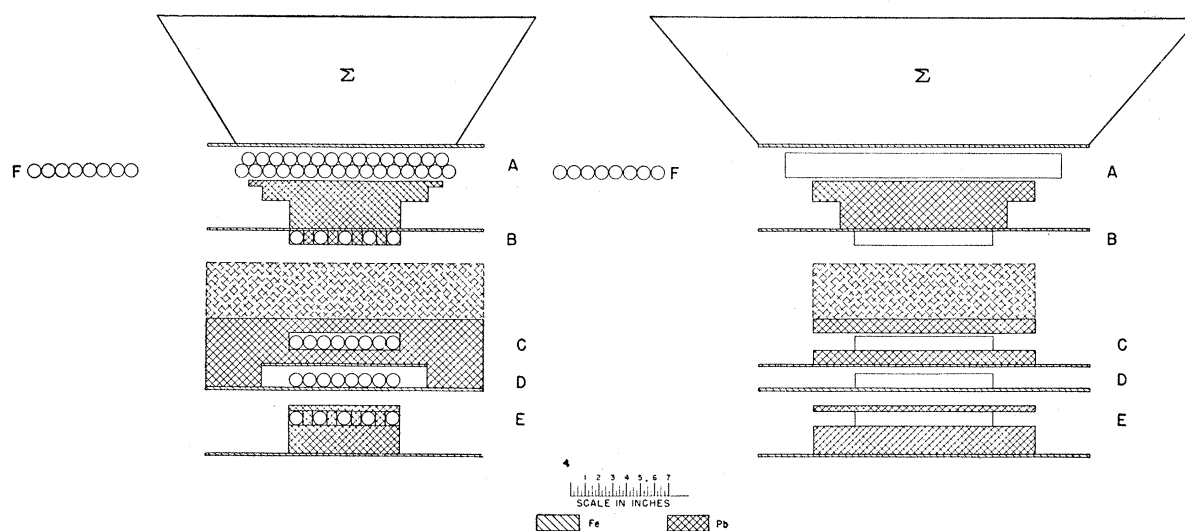


FIG. 1. Experimental arrangement of counters and absorbers.

* This work was supported in part by the joint program of the ONR and AEC.

† Now on leave at Massachusetts Institute of Technology, Cambridge, Massachusetts.

¹ B. Rossi and V. H. Regener, *Phys. Rev.* **58**, 837 (1940).

² L. Janosy and G. D. Rochester, *Proc. Roy. Soc. (London)* **A182**, 180 (1943).

³ Walker, Walker, and Greisen, *Phys. Rev.* **80**, 546 (1950).

TABLE I. Penetrating shower rates for event P_{21} .

Absorber Σ g/cm ²	Detector penetration	$P_{21}-A$ counts/hr	$P_{21}F-A$ counts/hr	$P_{21}-A-F$ counts/hr	Barom. corr. factor	$P_{21}-A-F(\text{corr})$ counts/hr
Zero	I	8.67	0.23	8.44±0.27	0.982	8.29±0.27
Zero	II	4.83	0.17	4.67±0.13	0.973	4.54±0.13
36 g/cm ² C	I	5.60	0.22	5.38±0.23	1.003	5.40±0.23
36 g/cm ² C	II	3.11	0.11	3.00±0.15	0.968	2.90±0.15
72 g/cm ² C	I	4.34	0.25	4.08±0.16	1.030	4.20±0.16
72 g/cm ² C	II	2.50	0.11	2.39±0.11	0.985	2.35±0.11
108 g/cm ² C	I	3.09	0.25	2.84±0.14	1.080	3.07±0.14
108 g/cm ² C	II	1.82	0.12	1.70±0.10	0.979	1.66±0.10
5 g/cm ² Fe	I	8.05	0.60	7.45±0.61	1.041	7.76±0.61
28.5 g/cm ² Pb+5 g/cm ² Fe	I	6.92	0.52	6.40±0.50	1.018	6.52±0.50
57 g/cm ² Pb+5 g/cm ² Fe	I	5.74	0.39	5.35±0.42	1.009	5.40±0.42
171 g/cm ² Pb+5 g/cm ² Fe	I	3.92	0.15	3.77±0.31	1.062	4.00±0.31
285 g/cm ² Pb+5 g/cm ² Fe	I	2.99	0.17	2.82±0.23	1.041	2.94±0.23

TABLE II. Penetrating shower rates for event P_{22} .

Absorber Σ g/cm ²	Detector penetration	$P_{22}-A$ counts/hr	$P_{22}F-A$ counts/hr	$P_{22}-A-F$ counts/hr	Barom. corr. factor	$P_{22}-A-F(\text{corr})$ counts/hr
Zero	I	2.42	0.11	2.31±0.14	0.982	2.27±0.14
Zero	II	1.11	0.07	1.04±0.06	0.973	1.01±0.06
36 g/cm ² C	I	1.44	0.11	1.33±0.12	1.003	1.33±0.12
36 g/cm ² C	II	0.66	0.02	0.64±0.07	0.968	0.62±0.07
72 g/cm ² C	I	1.10	0.09	1.01±0.08	1.030	1.04±0.08
108 g/cm ² C	I	0.92	0.10	0.82±0.08	1.080	0.89±0.08
108 g/cm ² C	II	0.32	0.04	0.28±0.04	0.979	0.27±0.04
5 g/cm ² Fe	I	2.50	0.45	2.05±0.32	1.041	2.13±0.32
28.5 g/cm ² Pb+5 g/cm ² Fe	I	1.96	0.20	1.76±0.27	1.018	1.79±0.27
57 g/cm ² Pb+5 g/cm ² Fe	I	1.77	0.19	1.58±0.23	1.009	1.59±0.23
171 g/cm ² Pb+5 g/cm ² Fe	I	1.04	0.08	0.96±0.16	1.062	1.02±0.16
285 g/cm ² Pb+5 g/cm ² Fe	I	0.63	0.10	0.53±0.10	1.041	0.55±0.10

TABLE III. Penetrating shower rates for event P_{32} .

Absorber Σ g/cm ²	Detector penetration	$P_{32}-A$ counts/hr	$P_{32}F-A$ counts/hr	$P_{32}-A-F$ counts/hr	Barom. corr. factor	$P_{32}-A-F(\text{corr})$ counts/hr
Zero	I	0.92	0.04	0.88±0.09	0.982	0.86±0.09
Zero	II	0.43	0.01	0.42±0.04	0.973	0.41±0.04
36 g/cm ² C	I	0.48	0.01	0.47±0.07	1.003	0.47±0.07
36 g/cm ² C	II	0.23	0.00	0.23±0.04	0.968	0.22±0.04
72 g/cm ² C	I	0.30	0.01	0.29±0.04	1.030	0.30±0.04
72 g/cm ² C	II	0.21	0.01	0.20±0.03	0.985	0.20±0.03
108 g/cm ² C	I	0.28	0.03	0.25±0.04	1.080	0.27±0.04
108 g/cm ² C	II	0.11	0.01	0.10±0.02	0.979	0.10±0.02
5 g/cm ² Fe	I	0.75	0.00	0.75±0.20	1.041	0.78±0.20
28.5 g/cm ² Pb+5 g/cm ² Fe	I	0.88	0.04	0.84±0.20	1.018	0.86±0.20
57 g/cm ² Pb+5 g/cm ² Fe	I	0.52	0.03	0.49±0.13	1.009	0.49±0.13
171 g/cm ² Pb+5 g/cm ² Fe	I	0.28	0.00	0.28±0.08	1.062	0.30±0.08
285 g/cm ² Pb+5 g/cm ² Fe	I	0.10	0.00	0.10±0.05	1.041	0.10±0.05

penetrate 71 g cm⁻² of Pb plus 8.7 g cm⁻² of Fe, a detector penetration which will be referred to as I. An additional lead absorber could be inserted in the region shown by the broken cross-hatching in Fig. 1. In this condition, referred to as II, the total absorber in the detector consisted of 185 g cm⁻² of Pb plus 8.7 g cm⁻² of Fe. Range-energy curves indicate that a proton and π -meson must have kinetic energies in excess of about 255 Mev and 135 Mev, respectively, in order to penetrate detector I. In the case of detector II the proton and π -meson energies must exceed 440 Mev and 265 Mev, respectively. Heavy shielding was used wherever

possible to protect the trays from side showers. The $\frac{3}{4}$ -inch lead spacers which separated the counters in the B and E trays, and the layer of lead immediately over the E tray reduced the background that resulted from multiple electronic secondaries of μ -mesons. The equipment was operated in a trailer, at an altitude of 10,600 ft above sea level.

The events of interest in the measurements reported here were $B_m C D E_n$ coincidences that were unaccompanied by the discharge of tray A . Such events ($B_m C D E_n - A$), hereafter designated by $P_{mn} - A$, are presumably a result of high energy neutral particles

which traverse the absorber Σ and tray A undetected and produce nuclear interactions in the 100 g cm^{-2} lead layer located between tray A and tray B . The experimental method employed is similar to that of other investigators and consists in measuring the rate of occurrence of the above events as a function of the variable absorber thickness Σ . It is presumed that a high energy neutral particle, which undergoes a nuclear collision in the absorber, either disappears or if it survives the encounter produces secondary charged particles capable of discharging tray A . In both cases the incident particle can no longer give rise to a $P_{mn}-A$ event. On the other hand, a neutral particle that does not have a collision in the absorber is just as likely to produce a $P_{mn}-A$ event as if the absorber were not there. Thus from the rate of decrease of the counting rate with increasing absorber thickness, one can determine the collision mean free path of the high energy neutral particles in the material of the absorber.

In order to discriminate against spurious events caused by air showers, two extension trays, F , were placed at the sides of the penetrating shower detector (see Fig. 1) and coincidences, $P_{mn}F-A$, between the anticoincidences, $P_{mn}-A$, and the discharges of the F trays were recorded. The corresponding counting rate was then subtracted from the counting rate of the $P_{mn}-A$ events to obtain the corrected counting rate, $P_{mn}-A-F$. Admittedly this method of discrimination is open to criticism, since it may rule out events that should be accepted. For example, a neutron may produce in the lead below tray A a nuclear interaction in which a secondary charged particle is projected sideways through one of the F trays. The procedure used is justifiable only because the correction is small. In fact the most important purpose achieved by the use of the extension trays was to prove that air showers do not have a significant effect upon the present experiment.

It is apparent that inefficiency in the anticoincidence tray A would give rise to a troublesome constant background in the recorded anticoincidence rate. For this reason the counters in this tray were stacked in a double layer and divided into four groups with each group feeding its associated fast amplifier and output circuits. The pulses from the four groups were then mixed to form the total A tray output. In this manner serious inefficiency caused by the dead time of the amplifiers and output circuits was reduced to a minimum. Frequent measurements showed that the A tray had an efficiency of about 99.5 percent.

RESULTS

Tables I through IV present a summary of the data for the different events aforementioned. A barometric correction factor was used to normalize the data to the average barometric pressure during the experiment. This correction factor was based on an absorption

thickness of the N -component in air equal to 120 g cm^{-2} . The corrected data are plotted in Figs. 2 and 3. One sees that the absorption curves are exponential within the experimental errors. The solid lines represent data taken with detector penetration I while the dashed lines are the curves for the measurements with detector penetration II.

A complete summary of the results based on the assumption of exponential absorption and obtained by least square analysis is given in Table V. From this table one notices that the apparent mean free path decreases as the multiplicity in the penetrating shower increases. It is evident that higher multiplicity of the particles in the detected event corresponds, on the average, to a higher energy of the incident particle responsible for the event. Thus the results, if taken at face value, would indicate that the mean free path decreases as the energy of the particle producing the nuclear interaction increases. It is important to notice, however, that this effect may be of an instrumental character. For example, a high energy neutron on traversing the absorber Σ may undergo a nuclear interaction in which it loses only a small amount of energy and produces a few low energy charged particles. The charged particles may be stopped by ionization loss before they reach the anticoincidence tray A , while the neutron may go on to produce another nuclear interaction in the material below A . The occurrence of events such as the one described above would make the observed mean free path longer than the actual mean free path. It is reasonable to assume that this source of error is more effective at low neutron energies than at high neutron energies because, as the energy of the neutron increases, the penetration of the secondary charged particles produced in its nuclear interactions also increases. Thus the effect described may possibly explain the energy dependence of the observed mean free paths.

TABLE IV. Penetrating shower rates for event P_{31} .

Absorber Σ g/cm ²	Detector penetration	$P_{31}-A$ counts/hr	Barom. corr. factor	$P_{31}-A$ (corr.) counts/hr
Zero	I	2.29 ± 0.14	0.982	2.25 ± 0.14
Zero	II	1.35 ± 0.06	0.973	1.31 ± 0.06
36 g/cm ² C	I	1.28 ± 0.12	1.003	1.28 ± 0.12
36 g/cm ² C	II	0.88 ± 0.08	0.968	0.85 ± 0.08
72 g/cm ² C	I	1.04 ± 0.08	1.030	1.07 ± 0.08
72 g/cm ² C	II	0.62 ± 0.06	0.985	0.61 ± 0.06
108 g/cm ² C	I	0.74 ± 0.07	1.080	0.80 ± 0.07
108 g/cm ² C	II	0.46 ± 0.05	0.979	0.45 ± 0.05
5 g/cm ² Fe	I	2.05 ± 0.32	1.041	2.13 ± 0.32
28.5 g/cm ² Pb				
+5 g/cm ² Fe	I	2.20 ± 0.30	1.018	2.24 ± 0.30
57 g/cm ² Pb				
+5 g/cm ² Fe	I	1.40 ± 0.20	1.009	1.41 ± 0.20
171 g/cm ² Pb				
+5 g/cm ² Fe	I	0.86 ± 0.15	1.062	0.91 ± 0.15
285 g/cm ² Pb				
+5 g/cm ² Fe	I	0.61 ± 0.11	1.041	0.64 ± 0.11

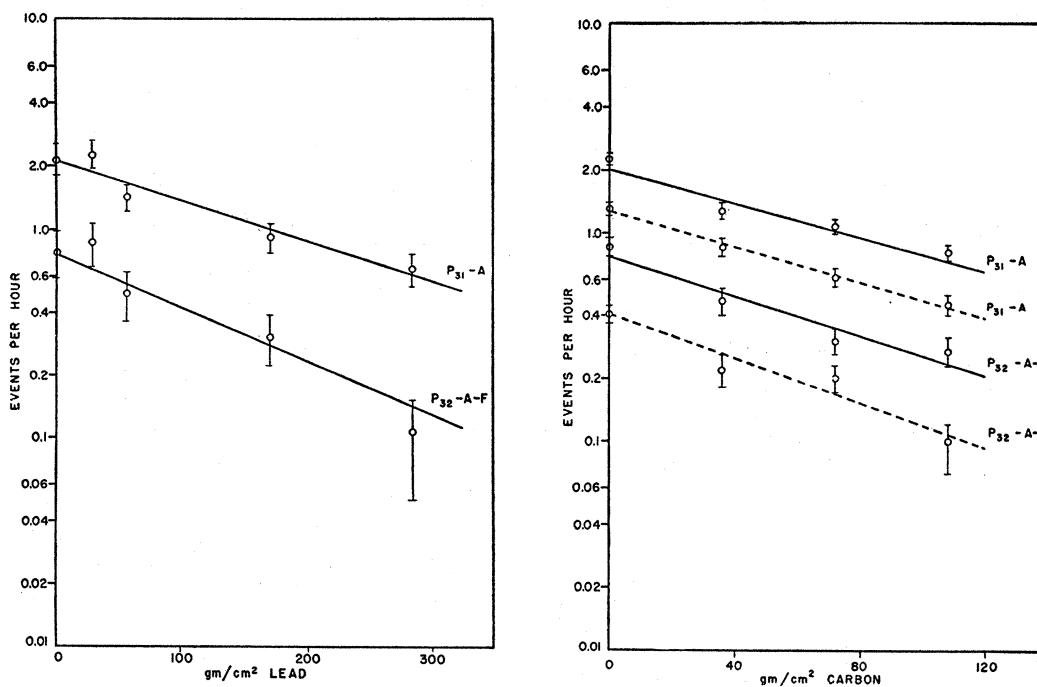


FIG. 2. The rate of occurrence of events $P_{21}-A-F$ and $P_{22}-A-F$ as a function of the thickness Σ of lead and carbon absorbers. The solid and dashed curves represent data with detector penetrations I and II, respectively.

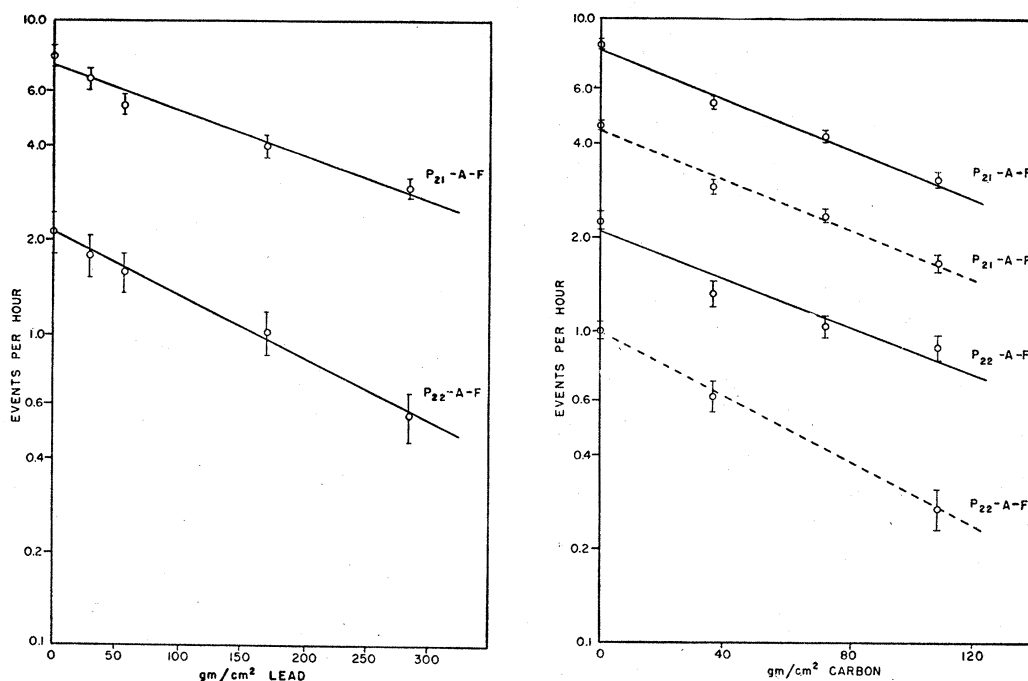


FIG. 3. The rate of occurrence of events $P_{31}-A$ and $P_{32}-A-F$ as a function of the thickness Σ of lead and carbon absorbers. The solid and dashed curves represent data with detector penetrations I and II, respectively.

The aforementioned arguments suggest that the most reliable determinations of the collision mean free path are those corresponding to events of highest multiplicity. Our experimental values for these mean free paths (see Table V) agree well with those obtained by

other authors (Walker, Walker, and Greisen).³ They are also consistent with the present views on the dimensions and structure of nuclei. In fact, if one assumes a nuclear radius $r_n = r_0 A^{1/3}$ (with $r_0 = 1.38 \times 10^{-13}$ cm and A equal to the atomic number), one finds that the geometrical

mean free path (i.e., the mean free path computed for completely opaque nuclei) is 165 g cm^{-2} in lead and 65 g cm^{-2} in carbon. One sees that the observed mean free path in lead comes close to the geometrical mean free path whereas the observed mean free path in carbon is somewhat longer than the geometrical mean free path. The obvious and reasonable conclusion is that the heavy lead nucleus is completely opaque to high energy neutrons whereas the light carbon nucleus is slightly transparent.

It may be noted that, if one considers instead the events of low multiplicity, the values of the observed mean free paths in lead and carbon are not consistent with the model of partially transparent nuclei. For example, the mean free paths corresponding to $P_{21}-A-F$ events is $108 \pm 6 \text{ g cm}^{-2}$ in carbon and $311 \pm 34 \text{ g cm}^{-2}$ in lead. According to the theory of Fernbach, Serber, and Taylor,⁴ 311 g cm^{-2} in lead corresponds to 245 g cm^{-2} in carbon. The disagreement confirms our previous assumption that, in the case of low multiplicity events, the mean free path measurements are falsified by the occurrence in the absorber of nuclear interactions in which the neutron survives and no ionizing particles are produced capable of discharging the anticoincidence tray A . For a given energy of the primary neutron, these events probably occur more frequently in lead than in carbon, because the secondary particles from a nuclear interaction in lead are presumably more numerous and less energetic than those arising from a similar interaction in carbon and have thus a greater probability of being reabsorbed before reaching tray A . If the above analysis is correct, one concludes that the difference between the observed and the actual mean free path is greater in lead than in carbon. This conclusion, qualitatively at least, explains the disagreement noted before.

A possible source of error is the production of penetrating showers by particles coming in at large angles from the vertical and thus reaching the lead below tray A without traversing the absorber Σ . Such particles could be either neutral or charged since a charged particle might conceivably strike the producing layer without passing through the anticoincidence tray A . This effect would contribute a background rate independent of the absorber thickness Σ and the observed

⁴ Fernbach, Serber, and Taylor, Phys. Rev. **75**, 1352 (1949).

TABLE V. Mean free paths.

Event	Absorber	Detector penetration	Mean free path (g cm ⁻²)
$P_{21}-A-F$	C	I	108 ± 6
$P_{21}-A-F$	C	II	108 ± 6
$P_{22}-A-F$	C	I	109 ± 11
$P_{22}-A-F$	C	II	81 ± 9
$P_{31}-A$	C	I	103 ± 10
$P_{31}-A$	C	II	98 ± 9
$P_{32}-A-F$	C	I	85 ± 12
$P_{32}-A-F$	C	II	85 ± 13
$P_{21}-A-F$	Pb	I	311 ± 34
$P_{22}-A-F$	Pb	I	220 ± 35
$P_{31}-A$	Pb	I	218 ± 34
$P_{32}-A-F$	Pb	I	143 ± 30

absorption curves would be of the form $N(x) = N_0 + N_0 e^{-x/L}$, where $N(x)$ is the counting rate at the absorber thickness, x , L is the mean free path, and N_0 and N_0 are constants. In the present experiment such a source of error did not appear to be serious since the counting rates exhibited a simple exponential variation within the limits of statistical accuracy (except perhaps for some of the carbon curves taken with detector penetration I).

The possibility of charge exchange represents another possible source of error. For instance, a proton in traversing the absorber may change into a neutron without giving rise to secondary particles of sufficient penetration to discharge the anticoincidence tray. In order to measure this effect an additional tray of counters was placed above the absorber Σ . For absorber thicknesses of approximately half a mean free path of carbon or lead it was found that less than 5 percent of the $P_{mn}-A$ events could be attributed to protons which undergo charge exchange in the absorber.

This experiment was performed at the Inter-University High Altitude Laboratory at Echo Lake, Colorado. The original instrumentation of the experiment was carried out by Dr. John Tinlot and Dr. Bernard Gregory. We are indebted to them for their initial experimental work to determine the feasibility of the method. It is a pleasure to acknowledge the support and encouragement given to us by Professor Bruno Rossi. We wish to thank both Professor Rossi and Professor R. W. Williams for helpful discussions concerning the results.